Pairing-Enhanced Regioselectivity: Synthesis of Alternating Poly(Lactic-*co*-Glycolic Acid) from Racemic Methyl-Glycolide

Yiye Lu and Geoffrey W. Coates*

Department of Chemistry and Chemical Biology, Baker Laboratory, Cornell University, Ithaca, New York 14853-1301, United States of America

ABSTRACT: Poly(lactic-*co*-glycolic acid) (PLGA) is used *in vivo* for various biomedical applications. Due to its biodegradability and biocompatibility, PLGA is uniquely suited for controlled drug delivery with parenteral administration. Previously, we have established the synthesis of isotactic, alternating PLGA from enantiopure starting materials. Here, to fill in the gap of the current field, we have developed the synthesis of syndioenriched, alternating PLGA from racemic methyl-glycolide (*rac*-MeG). The synthesis of alternating PLGA is accomplished by a highly regioselective ring-opening polymerization of *rac*-MeG with an optimized racemic aluminum catalyst. Mechanistic studies are carried out to elucidate the pairing-enhanced catalyst regio- and stereocontrol. Polymer sequence fidelity has been established by NMR investigations, confirming a high degree of alternation of comonomer sequence and moderate syndiotacticity within the backbone stereoconfiguration. The resulting syndioenriched material is amorphous, which will facilitate drug complexation behavior.

Introduction

Polymers are an integral component for various biomedical applications including drug delivery, tissue engineering, and implants.[1-5] In the field of controlled drug delivery, non-degradable polymers like polyacrylates, cellulose, and polyethylene glycol are compatible with oral and topical administration,[6-9] whereas degradable poly(lactic-*co*-glycolic acid) (PLGA) is an ideal candidate for parenteral controlled release.[10-12] Of all biopolymers, PLGA is distinct for its superior biocompatible nature and highly tunable biodegradability.[13] The mechanism of this chemically controlled drug delivery process is that an active pharmaceutical ingredient (API) is mixed in the polymer matrix, and the slow diffusion and polymer degradation *in vivo* results in the gradual release of the API.[14]

PLGA with an alternating sequence (Scheme 1) has demonstrated enhanced control of the degradation rate, and thus drug release kinetics, compared to PLGA with a random sequence.[15-17] Random PLGA generally exhibits drug release kinetics that are largely uncontrolled, demonstrating initial rapid degradation followed by late stage slow degradation.[18] In comparison, alternating PLGA results in linear, constant, and programmable degradation.[15] This is because the evenly distributed lactic (L) and glycolic (G) units make the hydrolytic attack a similar rate along the polyester backbone, with the absence of the faster hydrolyzing G–G linkages, or slower hydrolyzing L–L linkages throughout the whole degradation process.[17,19] One common drawback in the controlled delivery system with random PLGA is the initial burst release, resulting in an unnecessarily high or even toxic level of drug concentration.[20] In fact, the alternating PLGA may reduce the unpreferred initial burst release and enable the fine-tuning of API release kinetics.[15,20]

It is desirable to not only produce PLGA that is alternating in sequence but also amorphous in nature.[21] Semicrystalline PLGA is preferred for biomedical uses that require mechanical strength, while amorphous PLGA chains can be more flexible and better complex drug molecules (Scheme 1, top right).[18,22-24] The uniform degradation of alternating PLGA and homogeneous drug dispersion of amorphous PLGA combined, can become a great candidate for controlled drug delivery.[25]

Tacticity is another consideration for polymer crystallinity. PLGA may have isotactic, syndiotactic, and atactic microstructures, depending on the starting material chirality and the reaction stereoselectivity. The FDA has only approved applications containing PLGA that is derived from glycolide and racemic lactide comonomers for

Scheme 1. The synthesis of alternating PLGA with racemic and enantiopure monomers to synthesize materials for drug complexation

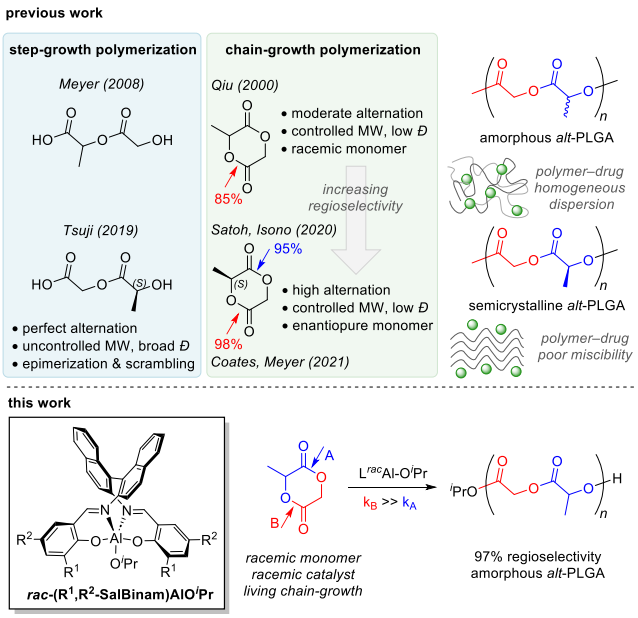

in vivo use as drug excipients.[10,26] This is because the isotactic PLGA made with enantiopure lactide is often semicrystalline or becomes semicrystalline during degradation.[15,27-29] While syndiotactic and atactic PLGA both remain amorphous, it has been reported that the syndiotactic PLGA has the lowest T_g, as compared to atactic and isotactic PLGA with the same composition.[30]

The synthesis of alternating PLGA has only been reported via a few methods (Scheme 1, top left). The Meyer and Tsuji groups have reported the step-growth segmer assembly polymerization (SAP) of LG or GL segmers to precisely pre-install the alternating sequence within the monomer.[30-32] However, this method is uncontrolled and suffers from epimerization and scrambling up to 5%.[30] Alternatively, several groups have independently introduced regioselective ring-opening polymerization (ROP) of methyl-glycolide to achieve the alternating polymer sequence via a chain-growth mechanism (Scheme 1, top middle).[33-37] The regioselectivity can be tuned from 85% to 98% with different catalysts.

However, the controlled polymerization of methyl-glycolide to alternating PLGA with relatively high regioselectivities so far has only been demonstrated with enantiopure monomers. The resulting isotactic P*L*LGA polymer exhibits some extent of crystallinity, which can be desirable for application as biodegradable implants. In 2019, the Tsuji group initially showed the melting behavior of isotactic alternating PLGA, although the T_m was only present in the first differential scanning calorimetry (DSC) heating cycle.[32] In our previous report, the melting point increased with higher regioregularity, isotacticity, and molecular weight, with a T_m on first heat around 97 °C.[35] It was also reported that P*L*LGA formed a stereocomplex when mixed with its opposite configuration P*D*LGA to further increase T_m and crystallinity.[32,34]

The synthesis of highly alternating PLGA with amorphous morphology remains unexplored. Therefore, we were interested in the synthesis of amorphous, alternating PLGA from racemic methyl-glycolide (*rac*-MeG), to fill in the gap of the current field (Scheme 1, bottom). The motivation was to minimize polymer crystallinity and to potentially provide another promising candidate for controlled drug delivery. We hypothesized that our previous method of attaining alternating P*L*LGA with (*S*)-MeG could be adapted to *rac*-MeG. Salen–Al catalysts in general are well studied for ring-opening polymerizations.[38] Especially, chiral ligands can facilitate stereoselective catalysis.[39] However, the chiral *N,N'*-bis(salicylidene)-1,1'-binaphthyl-2,2'-diamine (SalBinam) ligand was less studied, albeit with excellent stereoselectivity in both small molecule transformations and polymerizations.[40-42] After catalyst optimization, we found a substituted racemic (SalBinam)AlO^{i}Pr catalyst could both ensure high regioselectivity by the exclusive ring-opening at the glycolyl site (Scheme 1, site B) and afford an amorphous syndiotactic-enriched polymer. The reaction conditions are mild and the polymerization proceeds in a controlled and living manner to target different molecular weights.

Results and Discussion

Previously, we were able to utilize the chirality mismatch strategy to perform the regioselective ring-opening polymerization of enantiopure (*S*)-MeG (regioselectivity = 98%).[35] The (*R*)-(SalBinam)AlO^{i}Pr catalyst was chirality-mismatched with the (*S*)-lactyl site, which prevented the ring-opening from the (*S*)-lactyl site.[43-45] However, when we moved from (*S*)-MeG to *rac*-MeG, the previous strategy no longer applied. Using this *R* catalyst on *rac*-MeG, the regioselectivity was reduced to 86% (Table 1, entry 1). Since there was always a 50:50 mixture of matched and mismatched catalyst–monomer pairs, ring-opening no longer occurred exclusively at the glycolyl site. Nevertheless, the high initial regioselectivity prompted us to modify the catalyst by adding ortho- and para-substituents to the phenol rings on the ligand and to investigate their effect on regioselectivity. We first began by altering catalyst electronics at the para-position of the phenol. However, changing the para-substitution

Table 1. Catalyst screening for regioselectivity and syndiotacticity optimization

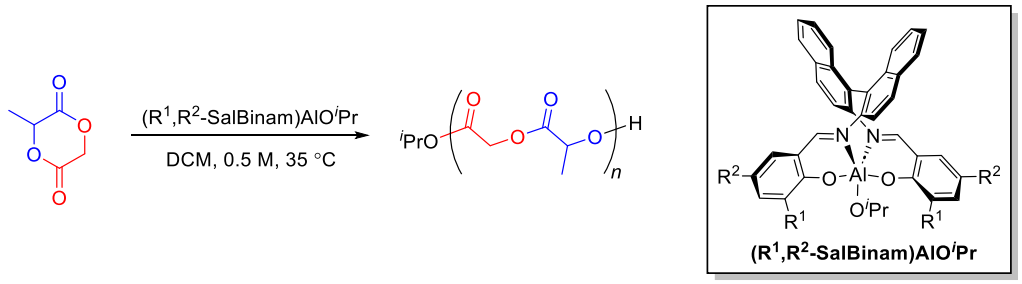

entry[a]	Binam chirality	R^1	R^2	time (h)	conv. (%)[b]	$M_{n\,theo}$ (kDa)	$M_{n\,GPC}$ (kDa)[c]	$Đ$[c]	regioselectivity (%)[b]	[mm]:[mr/rm]:[rr][d]	P_r[d]
1	*R*	H	H	23	91	11.9	15.7	1.05	86	26:50:24	0.49
2	*R*	H	OMe	22	89	11.6	14.2	1.06	86	27:49:24	0.49
3	*R*	Me	Me	24	75	9.8	11.9	1.04	92	24:47:29	0.54
4	*R*	^{t}Bu	^{t}Bu	25	9	1.1	1.9	1.10	n.d.[e]	n.d.[e]	n.d.[e]
5	*rac*	H	H	23	91	11.8	15.7	1.05	90	17:49:34	0.58
6	*rac*	Me	H	22	92	11.9	15.6	1.05	94	12:45:43	0.66
7	*rac*	Cl	Cl	24	59	7.7	16.6	1.06	95	3:31:66	0.81
8	*rac*	Ph	H	20	91	11.8	13.5	1.06	96	12:47:41	0.64
9	*rac*	Br	^{t}Bu	20	96	12.5	16.5	1.05	97	6:43:51	0.71

[a] [MeG]:[cat.] = 100:1. $[MeG]_0$ = 0.5 M. [b] Determined by ^{1}H NMR analysis. [c] Determined by GPC in THF, calibrated with polystyrene standards. [d] Determined by ^{13}C NMR analysis. [e] Not determined due to low molecular weight.

from H to a more electron-donating OMe group on the ligand had no effect on regioselectivity (Table 1, entry 2). As a result, we started to focus on altering the steric bulk at the ortho-position.

We hypothesized that altering the ortho group would change the steric environment during the coordination between the catalyst and incoming monomer, thereby impacting the regioselectivity. By switching the ortho group from H to a bulkier Me, the regioselectivity increased from 86% to 92% (Table 1, entry 3). Following this trend, we sought to further increase the steric bulk at the ortho position. Instead, changing the ortho-substituent to an even bulkier ^{t}Bu group dropped the reactivity significantly, yielding low molecular weight oligomers, which were challenging to characterize (Table 1, entry 4). These initial results suggest that the size of the ortho substituent may be tuned to optimize the regioselectivity, as long as it is not too large to inhibit polymerization.

We also observed that changing the catalyst backbone Binam chirality from *R* to racemic caused a consistent increase in regioselectivity (Table 1, entries 1, 3, 5 and 6). With the more selective racemic backbone, additional ortho-substituted catalysts were tried, of which the *ortho*-Br catalyst presented the highest regioselectivity (Table 1, entries 5–9 and Table S1). The regioselectivity increased with the steric environment change from H, Me, Cl, Ph, to Br substituent groups.[46] These results indicated that both too large or too small of an ortho substituent might reduce regioselectivity and that bromo had the optimized steric environment for the highest regioselectivity. The integrated steric effect, considering both substituent group size and distance to the ortho-carbon, needed to be experimentally determined. It is worth mentioning that the *para*-^{t}Bu group helped to increase the solubility and reactivity of the catalyst, whereas a relative electron withdrawing group, like Cl or NO_2, led to lower conversion or less efficient initiation (Table 1, entries 7 and 9, and Table S1, entry 2). This reaction was compatible with an alcohol chain transfer agent (CTA) to target a wide range of molecular weights or to install different chain ends, with similarly high regioselectivity (Table S1, entry 15). High molecular weight up to 34 kDa was also achieved with a high monomer loading (Table S1, entry 16). Large scale process development was accomplished and is described in supporting information (section 3.4). Interestingly, besides regioselectivity, we also observed syndioselectivity when we employed racemic monomer and racemic catalyst. The *di*-Cl catalyst exhibited the highest syndiotacticity, with a P_r of 0.81 (Table 1, entry 7), which will be described in detail in the mechanism later.

The NMR of the alternating PLGA polymer exhibits different peak patterns depending on the tacticity. When made from (*S*)-MeG, the resulting polymer is isotactic P*L*LGA, showing two methylene doublets between 4.6–4.9 ppm (Figure 1A). When made from *rac*-MeG, the resulting polymer demonstrates a syndiotactic-enriched pattern. The syndiotactic methylene doublets (*s*, 4.70 ppm and 4.82 ppm) have a different chemical shift from the isotactic methylene doublets (*i*, 4.64 ppm and 4.88 ppm).[30] The integration of *s* peaks is larger than that of *i* peaks as a result of being a syndioenriched polymer, which can also be confirmed with ^{13}C NMR integration (Figure S5). With the unsubstituted *R* catalyst, the polymerization achieves only moderate regioselectivity and thus moderately alternating PLGA. The extra peaks around 4.75–4.80 ppm and the low-intensity peaks around the baseline indicate the regiodefect.

In order to calculate the regioselectivity, we decided to start from the most sensitive ^{1}H NMR methylene region, using band-selective heteronuclear single quantum coherence (HSQC) experiment (Figure 1B) and heteronuclear multiple bond correlation (HMBC) experiment (Figure S62). Based on the three-bond correlation in HMBC and one-bond correlation in HSQC (Figure S8), we were able to assign the middle peaks (in red frame of Figure 1B) as the methylene peaks with regio-inversed sequence (red G). The chemical shifts of the two neighboring CH_2 (blue G and green G), though in the correct sequence, are also affected by the inversed sequence. There forms three sets of minor CH_2 (red, blue, green G) with one regio-inversed insertion (red G), the integration of which are in a

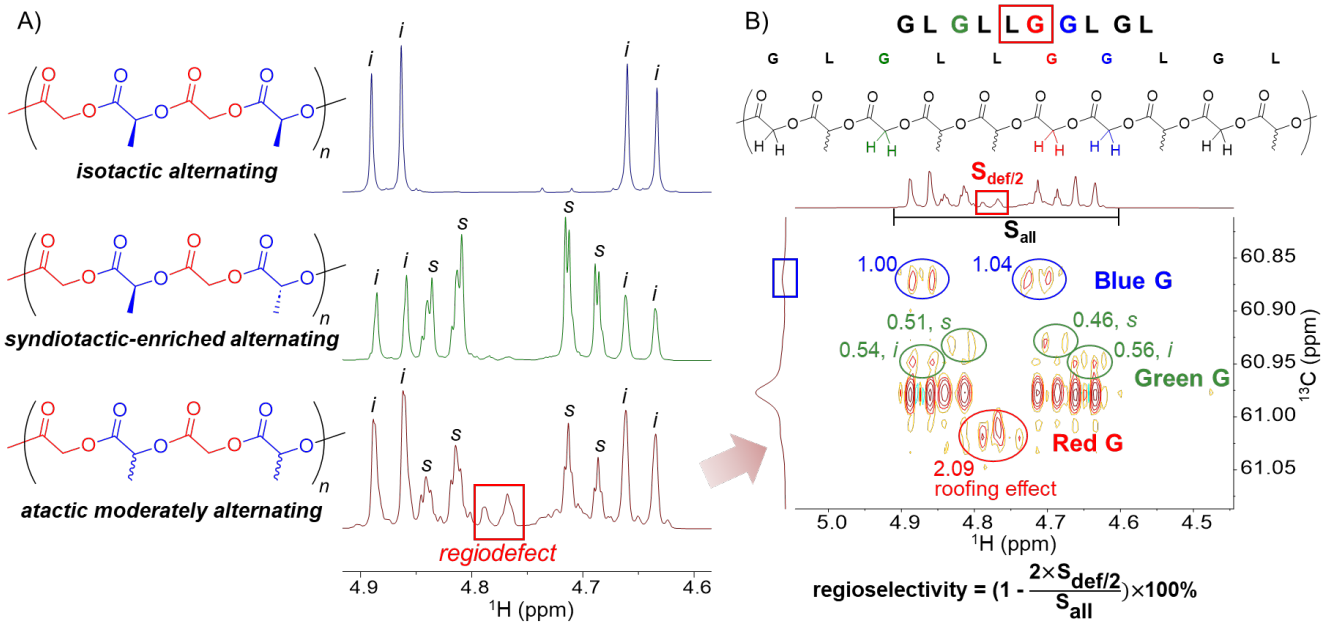

Figure 1. A) ^{1}H NMR spectra of alternating PLGA with different microstructures. *m*: CH_2 between two lactic units with the same stereoconfiguration; *r*: CH_2 between two lactic units with opposite stereoconfiguration. B) Band selective HSQC on the CH_2 region of atactic moderately alternating PLGA with regiodefect assignments and regioselectivity calculation.

1:1:1 ratio. Their chemical shifts can be assigned from HSQC accordingly. It is noteworthy that the green G splits into four doublets because there are two adjacent methyl groups next to the green CH_2, resulting in the isotactic (*i*, 4.64 ppm and 4.87 ppm) and syndiotactic (*s*, 4.69 ppm and 4.82 ppm) environment. The red G and blue G do not have two adjacent methyl on two sides and are not sensitive enough to feel the further distant tacticity difference, so they only split into two doublets. The red CH_2 manifests as two doublets very close in chemical shifts, which experience a slight roofing effect that increases the middle peaks intensity. Once we have fully assigned the peaks in the CH_2 region, the regioselectivity can be calculated by the integration of the blue G on ^{13}C NMR (blue frame), or the integration of the red G on ^{1}H NMR (red frame) (Figures S9–11). Since ^{13}C NMR is not as sensitive as ^{1}H NMR, it becomes less accurate to calculate high regioselectivity samples with a lower signal-to-noise ratio. We therefore opted to use integration based on the ^{1}H NMR red G to calculate regioselectivities. The integration of the middle two peaks gives half of the regiodefect CH_2 integration. The regioselectivity can then be calculated by comparing the defect CH_2 integration and the whole CH_2 region integration.

Intrigued by the effect of both substituent groups and catalyst chirality on regioselectivity, we pursued model studies of (*S*)- and *rac*-MeG, using *R*, *S*, and racemic catalysts with (H, H) and (Br, ^{t}Bu) ligands (Table 2). The *R* catalyst paired with (*S*)-MeG demonstrates the high regioselectivity (high regio%) pair. Likewise, *S* catalyst and (*S*)-MeG produces the low regioselectivity (low regio%) pair. When (*R*)-(H, H) catalyst reacts with *rac*-MeG, there is a 50:50 mixture of high regio% pair and low regio% pair, and thus the resulting regioselectivity (86%) is roughly a number average of high regio% (98%) and low regio% (78%) (Table 2, entries 1–3). This averaged regio% trend is an intrinsic chirality-resulted selectivity, which is once again observed with the (Br, ^{t}Bu) catalyst (Table 2, entries 5–7). Moreover, the obvious advance with the (Br, ^{t}Bu) catalyst is an increase in regioselectivity of the low regio% pair from 78% to 92%, which largely increases the overall performance in the reaction with *rac*-MeG (Figures 2A, S6, and S7). We attribute the increase of regioselectivity with (Br, ^{t}Bu) catalyst mainly to the steric hindrance created by the *ortho*-Br substituent. The steric hindrance further reduces the chirality-matched ring-opening at the unpreferred lactyl site (Figure 2A, site C), thus increasing the overall regioselectivity at the glycolyl site (Figure 2A, sites B and D).

Table 2. Regioselectivity study with original and optimized catalysts

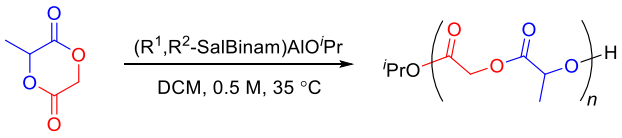

entry[a]	MeG chirality	Binam chirality	R^1	R^2	regioselectivity (%)[b]
1	*S*	*R*	H	H	98
2	*S*	*S*	H	H	78
3	*rac*	*R*	H	H	86
4	*rac*	*rac*	H	H	90
5	*S*	*R*	Br	^{t}Bu	98
6	*S*	*S*	Br	^{t}Bu	92
7	*rac*	*R*	Br	^{t}Bu	95
8	*rac*	*rac*	Br	^{t}Bu	97

[a] [MeG]:[cat.] = 100:1. $[MeG]_0$ = 0.5 M. [b] Determined by ^{1}H NMR analysis.

For both ligands, the reactions with *rac*-MeG both show an increased regioselectivity changing from the *R* catalyst to racemic catalyst (Table 2, entries 3, 4, 7, and 8). Now in the mixture of two monomers (*R* and *S*) and two catalysts (*R* and *S*), the cross combination can result in an even more complicated regioselectivity result. Since both the catalysts and monomers are mirror images of each other, we can simplify the combination to high regio% pair, low regio% pair, and the pair ratio between these two.

In the system with *R* catalyst and *rac*-MeG, there is always 50:50 *R* and *S* monomers; therefore, upon full monomer conversion, there is always a 50:50 pair ratio of high regio% pair (*R* catalyst with *S* monomer) and low regio% pair (*R* catalyst with *R* monomer) (Figure 2B, left). In the system with racemic catalyst and *rac*-MeG, the pair ratio is dependent on the chiral catalyst enantioselectivity preference. Kinetic resolution experiments reveal that *R* catalyst prefers *S* monomer over *R* monomer in a 3:1 ratio (k_{rel} = 3) with the (Br, ^{t}Bu) catalyst, and 2:1 with the (H, H) catalyst (k_{rel} = 2) (Figures S12–15). It is fortunate that the stereochemically preferred monomer is indeed the high regio% monomer. Therefore, the *rac*-(Br, ^{t}Bu) catalyst system has a higher pair ratio (75:25) than the *R*

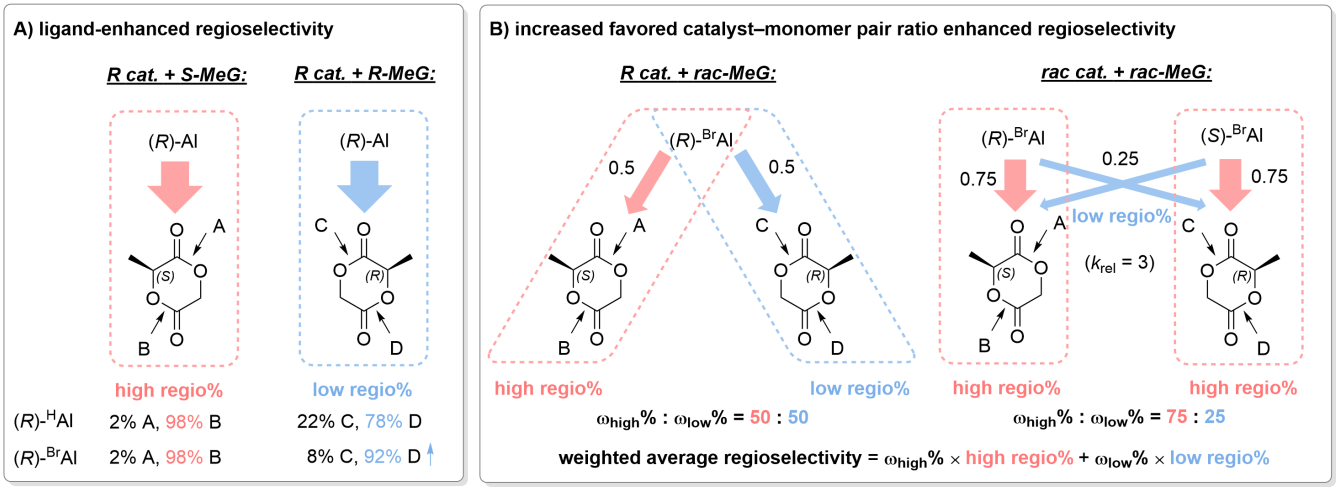

Figure 2. Optimization of catalyst ligand (A) and catalyst backbone chirality (B) to increase regioselectivity.

catalyst system (50:50) (Figure 2B, right). As a higher pair ratio corresponds to more ring-opening of the high regio% pair, higher regioselectivity is achieved with the racemic catalyst. The overall regioselectivity is now the weighted average of the high regio% pair and low regio% pair, considering the k_{rel} as the pair ratio (Figure 2B, bottom). Here, we observe a pairing-enhanced regioselectivity. With both enantiomers of catalyst and monomer in one pot, the monomer reservoir is always a racemic mixture. Each catalyst can always find its kinetically preferred high regio% monomer, rather than consuming the unpreferred low regio% monomer. The regioselectivity therefore remains constantly high throughout the entire reaction time. Notably, the second advance with the (Br, ^{t}Bu) catalyst is that by increasing k_{rel}, it increases the favored pair ratio and boosts the pairing-enhanced effect, subsequently increasing regioselectivity.

The overall high regioselectivity can be attributed to both the ligand-enhanced effect and the pairing-enhanced effect. The chain propagation with *rac*-MeG involves two steps: (1) selection of an *R*/*S* monomer (stereoselective); (2) selection of a G/L site (regioselective). Both steps can make a difference on overall regioselectivity. Step 1 monomer selection is influenced by the catalyst–monomer pair ratio, which increases the regioselectivity with the use of racemic catalyst and high k_{rel} ligand. Step 2 site selection is intrinsic to the ligand structure. Introduction of the *ortho*-Br substituent creates an appropriate steric effect that reduces the unpreferred ring-opening.

We also observed a syndiotacticity increase during the initial regioselectivity optimization, but only with racemic catalyst (Table 1, entries 5–9). In the case of *R* catalyst with *rac*-MeG, a single catalyst species initiates a polymer chain and the two monomer enantiomers join during the propagation. However, the kinetic resolution k_{rel} is not large enough to build much isotacticity. In the case of *rac*-(Br, ^{t}Bu) catalyst with *rac*-MeG, two catalyst species (*R* and *S*) will both initiate and consume their preferred monomer in a 3:1 ratio. Nevertheless, the ring-opening of the preferred monomer will lead to an unstable coordination in which the catalytic center and ring-opened chain end have opposite configurations (Scheme 2). As the *S*-ring-opened chain end is unstable with the *R* catalytic center, polymer exchange with the *S* catalytic center will occur to form a more stable coordination between *S* chain end and *S* catalyst. The new *S*-chain with the *S* catalyst will incorporate the next monomer with a 3:1 preference on the (*R*)-MeG, which leads to the syndiotactic nature of the polymer. This polymer exchange towards the more stable chain ends was also reported in the *meso*-LA regioselective ring-opening polymerization to form heterotactic PLA.[42] Since the k_{rel} is not substantially high, the polymer is only syndiotactic-enriched. Both polymer exchange and kinetic resolution need to be involved to build this unconventional syndiotacticity. Again, we observe this pairing-enhanced syndioselectivity, which requires the involvement of both enantiomers of the catalyst and monomer in pairs.

Although with high stereo- and regioregularity, all of these alternating PLGA samples remain amorphous, with no melting peak observed even on the first heat. The DSC has shown that the polymers have a glass transition temperature in a range of 44–48 °C (Table S2 and Figures S16–19). High regioselectivity tends to give a higher T_g, whereas high syndiotacticity leads to lower T_g. Furthermore, the alternating monomer sequence prevents the aggregation of L units or G units, which helps reduce the potential crystallinity that is unavoidable with the conventional method of copolymerizing lactide and glycolide.[47] As a result, we expect that the amorphous nature of the polymer and its highly alternating L/G microstructure will be beneficial for polymer–drug complexation and controlled drug delivery purposes.

Conclusions

In this work, we were able to synthesize alternating PLGA from racemic monomer and racemic catalyst to avoid polymer crystallinity. We investigated the steric effect of ortho substituents, electronic effect of para substituents, and pairing-enhanced effect of the racemic catalyst backbone. With the optimized catalyst, the polymer has near-perfect alternating L and G sequence and decently high syndiotacticity. We identified the origins of a pairing-enhanced regioselectivity and syndioselectivity with mechanistic studies. Compared to previous work, we were able to expand the scope of alternating PLGA from isotactic to syndiotactic, with a controlled chain-growth ring-opening polymerization method. This alternating PLGA made with racemic monomer remains amorphous, which is a good candidate for controlled drug delivery with homogeneous drug dispersion.

Future work will investigate the relationship between regioselectivity, tacticity, and polymer properties. The degradation study of this alternating PLGA with different molecular weights and tacticity is ongoing. We are also interested in studying detailed mechanisms of the polymer exchange process, the steric effect of ortho-substitution, and the regioselective mechanism with DFT calculations. Catalyst development for more isoselective or syndioselective polymerization from the racemic mixture is intriguing to us. With the

Scheme 2. Ring-opening mechanism for the origin of syndiotacticity

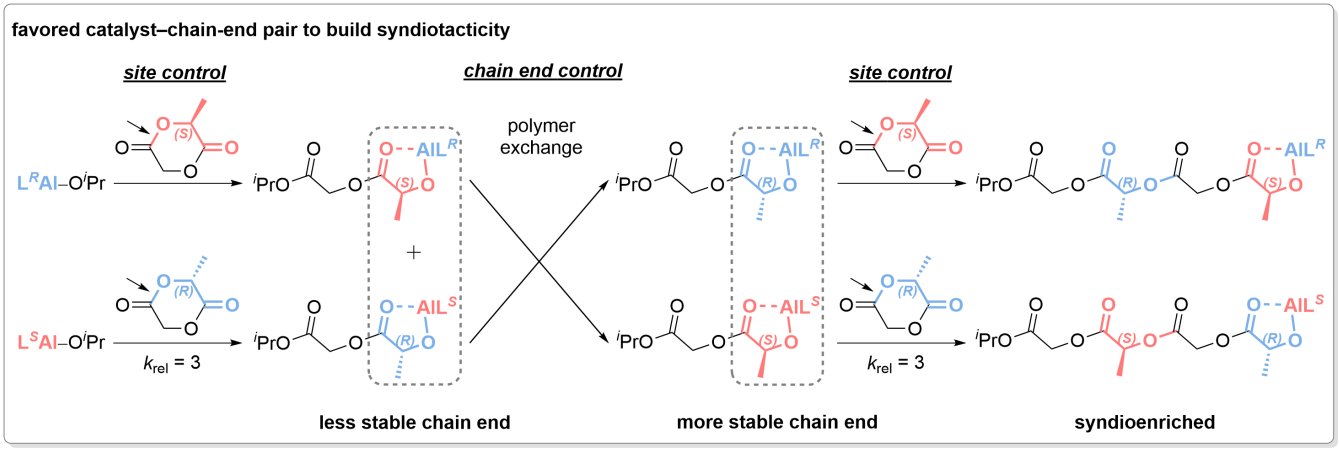

excellent stereoselectivity of this chiral SalBinam catalyst, we would like to extend the monomer scope to other lactones as well.

ASSOCIATED CONTENT

Supporting Information

This material is available free of charge via the Internet at http://pubs.acs.org.

Experimental procedures, material characterization and spectral data (PDF)

AUTHOR INFORMATION

Corresponding Author

Geoffrey W. Coates – Department of Chemistry and Chemical Biology, Baker Laboratory, Cornell University, Ithaca, New York 14853-1301, United States; orcid.org/0000-0002-3400-2552; Email: coates@cornell.edu

Author

Yiye Lu – Department of Chemistry and Chemical Biology, Baker Laboratory, Cornell University, Ithaca, New York 14853-1301, United States; orcid.org/0000-0002-6702-1258

Complete contact information is available at: http://pubs.acs.org.

Notes

Y.L. and G.W.C. are inventors on international patent WO2022173994A1, submitted by Cornell University, which covers the ring-opening polymerization of methyl-glycolide and synthesis of alternating PLGA.

ACKNOWLEDGMENT

This research was supported by the Center for Sustainable Polymers, a National Science Foundation (NSF) Center for Chemical Innovation (CHE-1901635) and Cornell University. This work made use of the NMR Facility at Cornell University, which is supported, in part, by the NSF under the award CHE-1531632. The authors thank Dr. Ivan Keresztes for assistance with NMR analysis.

REFERENCES

(1) Kamaly, N.; Yameen, B.; Wu, J.; Farokhzad, O. C. Degradable Controlled-Release Polymers and Polymeric Nanoparticles: Mechanisms of Controlling Drug Release. *Chem. Rev.* **2016**, *116*, 2602–2663.

(2) Green, J. J.; Elisseeff, J. H. Mimicking biological functionality with polymers for biomedical applications. *Nature* **2016**, *540*, 386–394.

(3) Ulery, B. D.; Nair, L. S.; Laurencin, C. T. Biomedical applications of biodegradable polymers. *J. Polym. Sci., Part B: Polym. Phys.* **2011**, *49*, 832–864.

(4) Gentile, P.; Chiono, V.; Carmagnola, I.; Hatton, P. V. An overview of poly(lactic-*co*-glycolic) acid (PLGA)-based biomaterials for bone tissue engineering. *Int. J. Mol. Sci.* **2014**, *15*, 3640–3659.

(5) Ekladious, I.; Colson, Y. L.; Grinstaff, M. W. Polymer–drug conjugate therapeutics: advances, insights and prospects. *Nat. Rev. Drug Discov.* **2019**, *18*, 273–294.

(6) Tao, S. L.; Lubeley, M. W.; Desai, T. A. Bioadhesive poly(methyl methacrylate) microdevices for controlled drug delivery. *J. Control. Release* **2003**, *88*, 215–228.

(7) Li, J.; Mooney, D. J. Designing hydrogels for controlled drug delivery. *Nat. Rev. Mater.* **2016**, *1*, 16071.

(8) Kathe, K.; Kathpalia, H. Film forming systems for topical and transdermal drug delivery. *Asian J. Pharm. Sci.* **2017**, *12*, 487–497.

(9) Ciolacu, D. E.; Nicu, R.; Ciolacu, F. Cellulose-Based Hydrogels as Sustained Drug-Delivery Systems. *Materials* **2020**, *13*, 5270.

(10) Park, K.; Skidmore, S.; Hadar, J.; Garner, J.; Park, H.; Otte, A.; Soh, B. K.; Yoon, G.; Yu, D.; Yun, Y.; Lee, B. K.; Jiang, X.; Wang, Y. Injectable, long-acting PLGA formulations: Analyzing PLGA and understanding microparticle formation. *J. Control. Release* **2019**, *304*, 125–134.

(11) Ibrahim, T. M.; El-Megrab, N. A.; El-Nahas, H. M. An overview of PLGA *in-situ* forming implants based on solvent exchange technique: effect of formulation components and characterization. *Pharm. Dev. Technol.* **2021**, *26*, 709–728.

(12) Benhabbour, S. R.; Kovarova, M.; Jones, C.; Copeland, D. J.; Shrivastava, R.; Swanson, M. D.; Sykes, C.; Ho, P. T.; Cottrell, M. L.; Sridharan, A.; Fix, S. M.; Thayer, O.; Long, J. M.; Hazuda, D. J.; Dayton, P. A.; Mumper, R. J.; Kashuba, A. D. M.; Victor Garcia, J. Ultra-long-acting tunable biodegradable and removable controlled release implants for drug delivery. *Nat. Commun.* **2019**, *10*, 4324.

(13) Makadia, H. K.; Siegel, S. J. Poly Lactic-*co*-Glycolic Acid (PLGA) as Biodegradable Controlled Drug Delivery Carrier. *Polymers (Basel)* **2011**, *3*, 1377–1397.

(14) Adepu, S.; Ramakrishna, S. Controlled Drug Delivery Systems: Current Status and Future Directions. *Molecules* **2021**, *26*, 5905.

(15) Li, J.; Rothstein, S. N.; Little, S. R.; Edenborn, H. M.; Meyer, T. Y. The effect of monomer order on the hydrolysis of biodegradable poly(lactic-*co*-glycolic acid) repeating sequence copolymers. *J. Am. Chem. Soc.* **2012**, *134*, 16352–16359.

(16) Li, J.; Stayshich, R. M.; Meyer, T. Y. Exploiting sequence to control the hydrolysis behavior of biodegradable PLGA copolymers. *J. Am. Chem. Soc.* **2011**, *133*, 6910–6913.

(17) Washington, M. A.; Swiner, D. J.; Bell, K. R.; Fedorchak, M. V.; Little, S. R.; Meyer, T. Y. The impact of monomer sequence and stereochemistry on the swelling and erosion of biodegradable poly(lactic-*co*-glycolic acid) matrices. *Biomaterials* **2017**, *117*, 66–76.

(18) Hines, D. J.; Kaplan, D. L. Poly(lactic-co-glycolic) Acid–Controlled-Release Systems: Experimental and Modeling Insights. *Crit. Rev. Ther. Drug Carrier Syst.* **2013**, *30*, 257–276.

(19) Vey, E.; Rodger, C.; Booth, J.; Claybourn, M.; Miller, A. F.; Saiani, A. Degradation kinetics of poly(lactic-co-glycolic) acid block copolymer cast films in phosphate buffer solution as revealed by infrared and Raman spectroscopies. *Polym. Degradation Stab.* **2011**, *96*, 1882–1889.

(20) Yoo, J.; Won, Y.-Y. Phenomenology of the Initial Burst Release of Drugs from PLGA Microparticles. *ACS Biomater. Sci. Eng.* **2020**, *6*, 6053–6062.

(21) Gilding, D. K.; Reed, A. M. Biodegradable polymers for use in surgery—polyglycolic/poly(lactic acid) homo- and copolymers: 1. *Polymer* **1979**, *20*, 1459–1464.

(22) Shi, N.-Q.; Lei, Y.-S.; Song, L.-M.; Yao, J.; Zhang, X.-B.; Wang, X.-L. Impact of amorphous and semicrystalline polymers on the dissolution and crystallization inhibition of pioglitazone solid dispersions. *Powder Technol.* **2013**, *247*, 211–221.

(23) Lanao, R. P. F.; Jonker, A. M.; Wolke, J. G. C.; Jansen, J. A.; van Hest, J. C. M.; Leeuwenburgh, S. C. G. Physicochemical Properties and Applications of Poly(lactic-co-glycolic acid) for Use in Bone Regeneration. *Tissue Eng. Part B Rev.* **2013**, *19*, 380–390.

(24) Pappalardo, D.; Mathisen, T.; Finne-Wistrand, A. Biocompatibility of Resorbable Polymers: A Historical Perspective and Framework for the Future. *Biomacromolecules* **2019**, *20*, 1465–1477.

(25) Šoljić Jerbić, I. Biodegradable Synthetic Polymers and their Application in Advanced Drug Delivery Systems (DDS). *Nano Tech Appl.* **2018**, *1*, 1–9.

(26) Wang, Y.; Qu, W.; Choi, S. H. FDA's Regulatory Science Program for Generic PLA/PLGA-Based Drug Products. *Am. Pharm. Rev.* **2016**, *19*, 5–9.

(27) Park, T. G. Degradation of poly(lactic-co-glycolic acid) microspheres: effect of copolymer composition. *Biomaterials* **1995**, *16*, 1123–1130.
(28) Blasi, P. Poly(lactic acid)/poly(lactic-co-glycolic acid)-based microparticles: an overview. *J. Pharm. Investig.* **2019**, *49*, 337–346.
(29) Xu, Y.; Kim, C.-S.; Saylor, D. M.; Koo, D. Polymer degradation and drug delivery in PLGA-based drug–polymer applications: A review of experiments and theories. *J. Biomed. Mater. Res. Part B: Appl. Biomater.* **2017**, *105*, 1692–1716.
(30) Stayshich, R. M.; Meyer, T. Y. New Insights into Poly(lactic-*co*-glycolic acid) Microstructure: Using Repeating Sequence Copolymers To Decipher Complex NMR and Thermal Behavior. *J. Am. Chem. Soc.* **2010**, *132*, 10920–10934.
(31) Stayshich, R. M.; Meyer, T. Y. Preparation and microstructural analysis of poly(lactic-*alt*-glycolic acid). *J. Polym. Sci., Part A: Polym. Chem.* **2008**, *46*, 4704–4711.
(32) Tsuji, H.; Yamasaki, M.; Arakawa, Y. Stereocomplex Formation between Enantiomeric Alternating Lactic Acid-Based Copolymers as a Versatile Method for the Preparation of High Performance Biobased Biodegradable Materials. *ACS Appl. Polym. Mater.* **2019**, *1*, 1476–1484.
(33) Dong, C.-M.; Qiu, K.-Y.; Gu, Z.-W.; Feng, X.-D. Synthesis of poly(D,L-lactic acid-*alt*-glycolic acid) from D,L-3-methylglycolide. *J. Polym. Sci., Part A: Polym. Chem.* **2000**, *38*, 4179–4184.
(34) Takojima, K.; Makino, H.; Saito, T.; Yamamoto, T.; Tajima, K.; Isono, T.; Satoh, T. An organocatalytic ring-opening polymerization approach to highly alternating copolymers of lactic acid and glycolic acid. *Polym. Chem.* **2020**, *11*, 6365–6373.
(35) Lu, Y.; Swisher, J. H.; Meyer, T. Y.; Coates, G. W. Chirality-Directed Regioselectivity: An Approach for the Synthesis of Alternating Poly(Lactic-*co*-Glycolic Acid). *J. Am. Chem. Soc.* **2021**, *143*, 4119–4124.
(36) Dong, C.-M.; Qiu, K.-Y.; Gu, Z.-W.; Feng, X.-D. Living polymerization of D,L-3-methylglycolide initiated with bimetallic (Al/Zn) μ-oxo alkoxide and copolymers thereof. *J. Polym. Sci., Part A: Polym. Chem.* **2001**, *39*, 357–367.
(37) Nifant'ev, I. E.; Shlyakhtin, A. V.; Bagrov, V. V.; Tavtorkin, A. N.; Komarov, P. D.; Churakov, A. V.; Ivchenko, P. V. Substituted glycolides from natural sources: preparation, alcoholysis and polymerization. *Polym. Chem.* **2020**, *11*, 6890–6902.
(38) MacDonald, J. P.; Shaver, M. P. Aluminum Salen and Salan Polymerization Catalysts: From Monomer Scope to Macrostructure Control. In *Green Polymer Chemistry: Biobased Materials and Biocatalysis*; American Chemical Society, 2015; pp 147–167.
(39) Gualandi, A.; Calogero, F.; Potenti, S.; Cozzi, P. G. Al(Salen) Metal Complexes in Stereoselective Catalysis. *Molecules* **2019**, *24*, 1716.
(40) Evans, D. A.; Aye, Y. Aluminum-Catalyzed Enantio- and Diastereoselective Carbonyl Addition of Propargylsilanes. A New Approach to Enantioenriched Vinyl Epoxides. *J. Am. Chem. Soc.* **2007**, *129*, 9606–9607.
(41) Hubbell, A. K.; Lamb, J. R.; Klimovica, K.; Mulzer, M.; Shaffer, T. D.; MacMillan, S. N.; Coates, G. W. Catalyst-Controlled Regioselective Carbonylation of Isobutylene Oxide to Pivalolactone. *ACS Catal.* **2020**, *10*, 12537–12543.
(42) Ovitt, T. M.; Coates, G. W. Stereochemistry of Lactide Polymerization with Chiral Catalysts: New Opportunities for Stereocontrol Using Polymer Exchange Mechanisms. *J. Am. Chem. Soc.* **2002**, *124*, 1316–1326.
(43) Spassky, N.; Wisniewski, M.; Pluta, C.; Le Borgne, A. Highly stereoelective polymerization of *rac*-(D,L)-lactide with a chiral schiff's base/aluminium alkoxide initiator. *Macromol. Chem. Phys.* **1996**, *197*, 2627–2637.
(44) Ovitt, T. M.; Coates, G. W. Stereoselective Ring-Opening Polymerization of *meso*-Lactide: Synthesis of Syndiotactic Poly(lactic acid). *J. Am. Chem. Soc.* **1999**, *121*, 4072–4073.
(45) Ovitt, T. M.; Coates, G. W. Stereoselective ring-opening polymerization of *rac*-lactide with a single-site, racemic aluminum alkoxide catalyst: Synthesis of stereoblock poly(lactic acid). *J. Polym. Sci., Part A: Polym. Chem.* **2000**, *38*, 4686–4692.
(46) Nomura, N.; Ishii, R.; Yamamoto, Y.; Kondo, T. Stereoselective Ring-Opening Polymerization of a Racemic Lactide by Using Achiral Salen– and Homosalen–Aluminum Complexes. *Chem. Eur. J.* **2007**, *13*, 4433–4451.
(47) Altay, E.; Jang, Y.-J.; Kua, X. Q.; Hillmyer, M. A. Synthesis, Microstructure, and Properties of High-Molar-Mass Polyglycolide Copolymers with Isolated Methyl Defects. *Biomacromolecules* **2021**, *22*, 2532–2543.

Table of Contents Graphic